



香港城市大學
City University of Hong Kong

專業 創新 胸懷全球
Professional · Creative
For The World

CityU Scholars

Deterministic generation and switching of dissipative Kerr soliton in a thermally controlled micro-resonator

Lu, Zhizhou; Wang, Weiqiang; Zhang, Wenfu; Chu, Sai T.; Little, Brent E.; Liu, Mulong; Wang, Leiran; Zou, Chang-Ling; Dong, Chun-Hua; Zhao, Bailing; Zhao, Wei

Published in:
AIP Advances

Published: 01/02/2019

Document Version:
Final Published version, also known as Publisher's PDF, Publisher's Final version or Version of Record

License:
CC BY

Publication record in CityU Scholars:
[Go to record](#)

Published version (DOI):
[10.1063/1.5080128](https://doi.org/10.1063/1.5080128)

Publication details:
Lu, Z., Wang, W., Zhang, W., Chu, S. T., Little, B. E., Liu, M., Wang, L., Zou, C-L., Dong, C-H., Zhao, B., & Zhao, W. (2019). Deterministic generation and switching of dissipative Kerr soliton in a thermally controlled micro-resonator. *AIP Advances*, 9(2), [025314]. <https://doi.org/10.1063/1.5080128>

Citing this paper

Please note that where the full-text provided on CityU Scholars is the Post-print version (also known as Accepted Author Manuscript, Peer-reviewed or Author Final version), it may differ from the Final Published version. When citing, ensure that you check and use the publisher's definitive version for pagination and other details.

General rights

Copyright for the publications made accessible via the CityU Scholars portal is retained by the author(s) and/or other copyright owners and it is a condition of accessing these publications that users recognise and abide by the legal requirements associated with these rights. Users may not further distribute the material or use it for any profit-making activity or commercial gain.

Publisher permission

Permission for previously published items are in accordance with publisher's copyright policies sourced from the SHERPA RoMEO database. Links to full text versions (either Published or Post-print) are only available if corresponding publishers allow open access.



Take down policy

Contact lbscholars@cityu.edu.hk if you believe that this document breaches copyright and provide us with details. We will remove access to the work immediately and investigate your claim.

Deterministic generation and switching of dissipative Kerr soliton in a thermally controlled micro-resonator

Cite as: AIP Advances 9, 025314 (2019); <https://doi.org/10.1063/1.5080128>

Submitted: 05 November 2018 . Accepted: 18 February 2019 . Published Online: 25 February 2019

Zhizhou Lu, Weiqiang Wang, Wenfu Zhang, Sai T. Chu, Brent E. Little, Mulong Liu, Leiran Wang, Chang-Ling Zou , Chun-Hua Dong, Bailing Zhao, and Wei Zhao 



View Online



Export Citation



CrossMark

ARTICLES YOU MAY BE INTERESTED IN

[Microcavity dispersion engineering for the visible optical frequency comb generation](#)

Applied Physics Letters **114**, 091104 (2019); <https://doi.org/10.1063/1.5080126>

[High performance RF filters via bandwidth scaling with Kerr micro-combs](#)

APL Photonics **4**, 026102 (2019); <https://doi.org/10.1063/1.5080246>

[Generation of multiple near-visible comb lines in an AlN microring via \$\chi^{\(2\)}\$ and \$\chi^{\(3\)}\$ optical nonlinearities](#)

Applied Physics Letters **113**, 171106 (2018); <https://doi.org/10.1063/1.5046324>

AVS Quantum Science

Co-published with AIP Publishing



Coming Soon!

Deterministic generation and switching of dissipative Kerr soliton in a thermally controlled micro-resonator

Cite as: AIP Advances 9, 025314 (2019); doi: 10.1063/1.5080128

Submitted: 5 November 2018 • Accepted: 18 February 2019 •

Published Online: 25 February 2019



Zhizhou Lu,^{1,2,a)} Weiqiang Wang,^{1,2,a),b)} Wenfu Zhang,^{1,2,c)} Sai T. Chu,³ Brent E. Little,¹ Mulong Liu,^{1,2} Leiran Wang,^{1,2} Chang-Ling Zou,^{4,5} Chun-Hua Dong,^{4,5} Bailing Zhao,^{4,5} and Wei Zhao^{1,2}

AFFILIATIONS

¹State Key Laboratory of Transient Optics and Photonics, Xi'an Institute of Optics and Precision Mechanics (XIOPM), Chinese Academy of Sciences (CAS), Xi'an 710119, China

²University of Chinese Academy of Sciences, Beijing 100049, China

³Department of Physics and Materials Science, City University of Hong Kong, Hong Kong, China

⁴Key Laboratory of Quantum Information, CAS, University of Science and Technology of China, Hefei, Anhui 230026, China

⁵Synergetic Innovation Center of Quantum Information & Quantum Physics, University of Science and Technology of China, Hefei, Anhui 230026, China

^{a)} **Contributions:** These authors contribute equally to this work.

^{b)} **Electronic mail:** wwq@opt.ac.cn

^{c)} **Electronic mail:** wfuzhang@opt.ac.cn

ABSTRACT

In this paper, we first experimentally demonstrate deterministic generation and switching of dissipative Kerr solitons (DKSs) in a thermally controlled micro-ring resonator based on high-index doped silica glass platform. In our scheme, an auxiliary laser is introduced to timely balance the intra-cavity heat fluctuation. By decreasing the operation temperature through a thermo-electric cooler, primary-, chaotic-comb and soliton crystal are firstly generated, then increasing the temperature, DKSs switching and single soliton are robustly accessed, which is independent of the tuning speed. During the switching process, varieties of DKSs are identified by tens of the characteristic “soliton-steps”. Besides, by simply changing the operation temperature under which the DKSs are formed, the center wavelength of dispersive waves could be tuned in a broadband range. When the micro-ring resonator operating at temperature larger than 63.5 °C, avoided mode-crossing free soliton can be obtained. Our results are favorable for study of on-chip soliton dynamics and practical nonlinear applications.

© 2019 Author(s). All article content, except where otherwise noted, is licensed under a Creative Commons Attribution (CC BY) license (<http://creativecommons.org/licenses/by/4.0/>). <https://doi.org/10.1063/1.5080128>

Micro-resonator-based dissipative Kerr solitons (DKSs) via parametric four-wave mixing (FWM) have drawn considerable interests in the last decade for its possibility of broad bandwidth, low power consumption and miniaturization operation.^{1,2} DKSs have been successfully demonstrated in MgF₂, Si₃N₄, Si, silica and AlN platforms,³⁻⁷ among which the spectra cover from visible to mid-infrared window and the repetition rate ranges from several gigahertz (GHz) to terahertz (THz).⁸ Up to now, DKSs have revolutionized the fields of dual-comb spectroscopy,^{9,10} chip-scale distance-ranging,^{11,12} low-noise microwave generation,¹³ optical

coherent communication system,^{14,15} and astrocomb-based optical calibration.^{16,17}

To realize practical applications, stably and deterministically accessing single-soliton state is the fundamental issue. While the generation of DKSs in a high-Q micro-cavity requires keeping the pump at effective red-detuned regime where the system suffers from thermal instability.¹⁸ Therefore, complicated techniques are developed to enable DKSs formation, such as rapid frequency tuning or two-protocol “power kicking” scheme,^{3,6} as well as rapid thermal-tuning method.¹⁹ However, the number of soliton formed in the

resonator is relatively stochastic.²⁰ Recently, H. Guo, et al. introduced a backward frequency tuning scheme to deterministically achieve single soliton state.²¹ Regrettably, this scheme relies on wavelength tunable laser which suffers from relatively high noise and broader linewidth typically on the order of $\sim 100\text{kHz}$. Recently, an auxiliary-laser-heating method is proposed to access and stabilize the DKS state.²² Within this scheme, an auxiliary laser is introduced to balance the thermal fluctuation inside the resonator. The intra-cavity heat reduction accompanying with the soliton state switching is compensated by the auxiliary laser which locates at the blue-detuned regime. Thus, the thermal instability is effectively alleviated and arbitrary laser detuning is allowed for the pump. However, in this scheme, the auxiliary and pump laser are in the same polarization state, thus the subsequent spectra-separation remains challenging, which restricts practical applications to some degree. Furthermore, the tunable laser is still required.

In this paper, we demonstrate deterministic DKSs generation and switching in a high-index doped silica glass micro-ring resonator (MRR)²³ using a thermo-electric cooler (TEC), which has been used to realize robust soliton crystal as presented in our previous work,²⁴ however, transition to single soliton is prohibited using single pump in our follow-up attempts. Here we introduce an auxiliary laser which is counter-coupled into the four-port MRR and orthogonally polarized compared with the pump. By sequentially decreasing and increasing the operation temperature, the DKS switching and annihilation could be clearly recognized from the optical spectra and characteristic discrete steps, which may help to research the intra-cavity soliton dynamics.²⁵ Additionally, it is convenient to separate the DKS from reflected auxiliary comb components using a polarization beam splitter (PBS), which could enable DKS-based applications and has been successfully used in quantum key distribution.²⁶ In a further proof experiment, we demonstrate that by setting the DKS-formed temperature, the center wavelength of dispersive waves (DW) could be easily tuned within a broadband range, and avoided mode-crossing free soliton comb can be obtained once the operation temperature is higher than 63.5°C .

Figure 1 shows the experimental set up for DKSs generation and switching, as well as spectra-separation. The monolithic

integrated four-port high-Q MRR is packaged in a butterfly-package with a thermo-electric cooler (TEC), as shown in the inset, where a Chinese 1 dime is for scaling. The ring radius is $\sim 592.1\mu\text{m}$, corresponding to the free spectral range (FSR) of $\sim 49\text{GHz}$.^{24,27} The cross-sections of the ring and bus waveguides are both $2\mu\text{m} \times 3\mu\text{m}$. The MRR exhibits anomalous dispersion in communication band.²⁸ The Q factors of TM_{00} mode (pump) and TE_{00} mode (auxiliary) are 2.05×10^6 and 1.69×10^6 , respectively.²⁸ The MRR is pigtailed with a standard fiber array with coupling loss of $\sim 2.5\text{dB}$ per facet²⁴ and insert loss from other passive optical devices of $\sim 1\text{dB}$. The operation temperature of the MRR can be precisely tuned through an external TEC controller. The pump laser (TM_{00} , ECDL #1) for soliton is a narrow-linewidth laser whose wavelength is 1561.792nm in our experiment while the auxiliary laser (TE_{00} , ECDL #2) is wavelength-tunable, allowing at least $1 \times \text{FSR}$ tuning range (0.4nm for this device). The two lasers are boosted to a similar power level (on-chip power of $31 \sim 33\text{dBm}$) using two commercial high-power erbium doped fiber amplifiers (EDFAs). Two fiber polarization controllers (FPCs) are used to control the polarization states of the two lasers. The circulators inhibit the strong light from transmitting to the EDFAs. The generated DKSs coupled out from the drop port are measured using two optical spectrum analyzers (OSAs), electrical spectrum analyzer (ESA) and oscilloscope (OSC).

In our experiments, the auxiliary and the pump laser are coupled into the orthogonal modes of the MRR simultaneously through carefully tuning the wavelength of the auxiliary laser, such as 1558.26nm in one of our tests. The pump laser is slightly closer to the corresponding resonance compared to the auxiliary laser while both of them are blue-detuned relative to each resonance. Fig. 2(a) sketches the complete evolution process of the intra-cavity optical spectra. Decreasing the operation temperature through the TEC, the pump first reaches the threshold of optical parametric oscillation (OPO). The primary and modulation instability (MI) combs are successively generated while the auxiliary laser keeps approaching the resonance but under the OPO threshold value (state (i) and (ii) of Fig. 2(a)). The corresponding experimental optical and electrical spectra are presented in state (i) and (ii) of Fig. 2(b), respectively. Further decreasing the temperature, the resonance climbs over the pump and the red-detuned regime is achieved, the corresponding optical spectrum exhibits soliton crystal feature (state (iii) of Figs 2(a) and (b)).^{24,29} During this process, the resulting power drop of pump comb inside the MRR is effectively compensated by the power increment of auxiliary laser which locates at blue-detuned regime. This is clearly proved by the complementary steps of power traces shown in Figs. 3(a) and (b), which are monitored via the drop- and add-port of the MRR. Further decreasing the temperature (forward tuning), the frequency combs will vanish as illustrated in Fig. 3(a). In contrast, increasing the temperature from this stage (backward tuning), the soliton switching could be stably accessed. This behavior is indicated in Fig. 3(b) where the number of solitons in the MRR is reduced step by step until single soliton state is achieved. State (iv) of Fig. 2 (b) shows the single soliton spectrum, where the sech^2 fitting (red) suggests 114fs pulse width and 4.4nm ($11 \times \text{FSR}$) frequency shift induced by Raman self-frequency shift (RSFS) and soliton recoil.³⁰ The RF spectra show $\sim 48.97\text{GHz}$ of repetition rate. Meanwhile, the discrete spikes comb lines reveals that the primary comb is stimulated simultaneously by the auxiliary

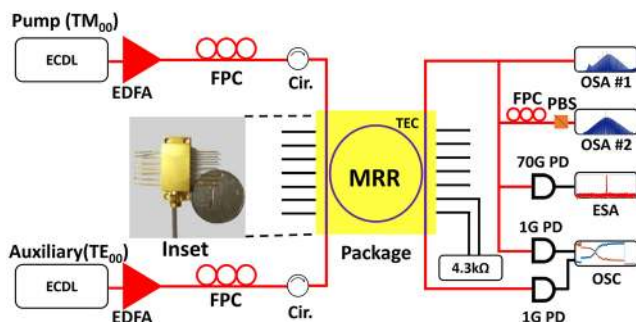


FIG. 1. Experimental set up for DKSs generation, switching behavior and comb-separation. The inset is the image of the packaged MRR used in the experiment. EDFA: erbium-doped fiber amplifier. FPC: fiber polarization controller. Cir: high power circulator. MRR: micro-ring resonator. PBS: polarization beam splitter. OSA: optical spectrum analyzer. OSC: oscilloscope. PD: photodetector. ESA: electrical spectrum analyzer.

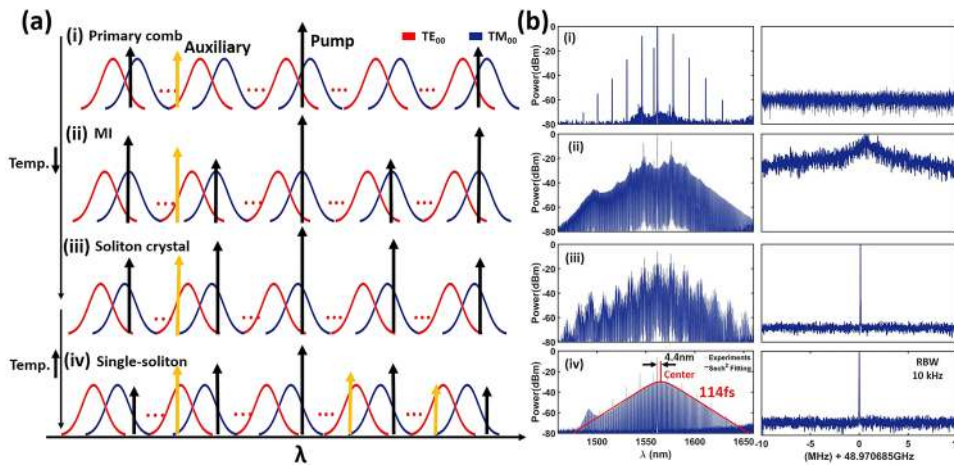


FIG. 2. DKS evolution with optical spectra and RF beat note. (a) Schematic diagram of DKS evolution. Decreasing the temperature (Temp.↓) from (i) primary comb, (ii) chaotic MI comb to (iii) soliton crystal state, then increasing the temperature ((Temp.↑)) until (iv) single soliton state is achieved. The corresponding optical and electrical spectra are shown in (b). The repetition rate of the single soliton is ~48.97 GHz with 4.4nm frequency shift and the pulse width is ~114fs. The pump and auxiliary laser are fixed while the resonances are shifted during the thermal tuning process.

laser. It should be noted that the state of the auxiliary comb is determined by the relative position of the pump and auxiliary lasers. These two combs are easily separated using a PBS in subsequent experiments.

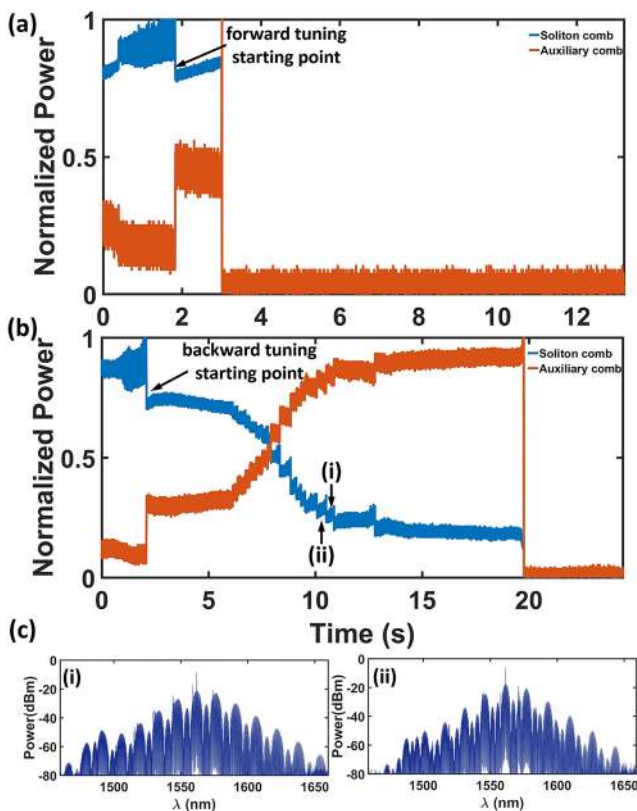


FIG. 3. The power trace under forward (a) and forward-backward tuning (b) schemes, the discrete steps suggest different soliton states, such as three- (i) and four- (ii) soliton state, whose spectra are shown as (i) and (ii) of (c), respectively.

It is intriguing that when the operation temperature is forward and backward tuned, the intra-cavity optical field exhibits entirely different feature. Such distinct observation is attributed to thermal nonlinearity in the MRR.²¹ Specifically, to maintain the soliton states, the frequency of the pump should keep in the soliton existence range (SER) ($\delta_L < \delta < \delta_H$), where δ_L and δ_H are the lower and upper boundaries of the SER, respectively. The upper boundary δ_H is degenerate with respect to the number of solitons.²¹ Therefore, DKSs switching can't be realized by increasing the effective detuning of the pump, which corresponds to decreasing the operation temperature in our scheme. On the contrary, the lower boundary of the SER is nondegenerate with respect to the number of solitons which benefits from the thermal nonlinearity²¹ of the high-Q MRR. Therefore, the staircase patterned power trace can be expected when the pump sweeps backward, equivalent to increasing the temperature in our experiments. Each step corresponds to a specific soliton state, as an example, the markers in Fig. 3 (b) are three- and four-soliton states whose spectra are shown as (i) and (ii) in Fig. 3(c), respectively.

In the optical spectrum of single soliton shown in Figs. 2(b), dispersive waves (DWs)³¹ are clearly observed at the wavelength of ~1490nm. We characterize the DW using a PBS, the pump and reflected auxiliary-comb spectra are presented in Figs. 4(a) and (b), respectively. It is clearly seen that the components of the DWs are almost in the same polarization with the auxiliary comb (TE mode). To investigate this situation, further integrated dispersion calculations are performed and shown in Fig. 4(c), where unperturbed (dashed line, no mode crossing) and perturbed (solid line, mode crossing) dispersion curves are both presented for comparison. During the calculation, the thermal-optic effect is considered and the coupling factor G is assumed to be $2\pi \times 500\text{MHz}$.³¹ The good match between calculation and experiment reveals that the TE₀₁ mode is involved as interacting mode and strong mode-interaction³² between TE₀₁ and TM₀₀ mode occurred inside the MRR, which leads to an avoided mode crossing on the mode dispersion curve (dashed line) that induces the DWs and mode hybridizations.³¹ Therefore the DW components in our device are expected to be in TE₀₁ mode.

To determine the Raman property as well as characterizing the temporal profile of different soliton states, we performed the

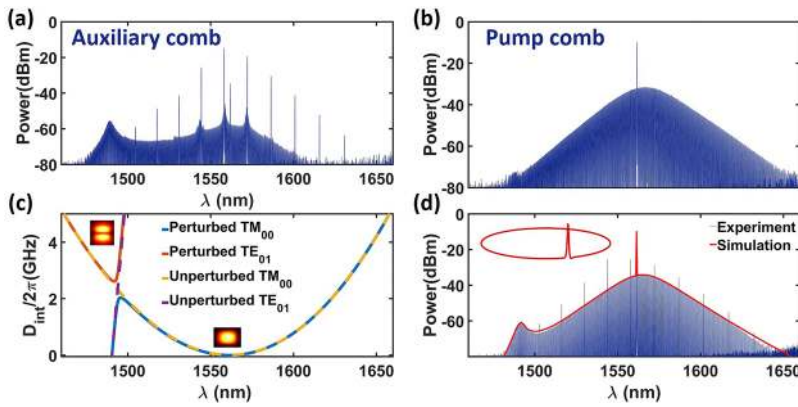


FIG. 4. DWs characterization and simulation. Reflected auxiliary (a) and pump (b) comb after PBS separation. DWs in same polarization with auxiliary comb. (c) Simulated integrated dispersion curves for TM_{00} and TE_{01} mode families, which qualitatively characterize the DW. Dash and solid lines shows unperturbed and perturbed modes, respectively. (d) Simulated (red) and experimental (midnight blue) spectra, showing good agreement. The inset is the simulated soliton pulse.

simulation using the damped, driven Lugiato-Lefever equation (LLE) with simplified Raman term in first order of Taylor expansion,^{33,34} which is valid in our case because the pulse width of 114fs of our device is larger than 100fs.³⁴⁻³⁶

$$\begin{aligned} (t_R \frac{\partial}{\partial t} + \frac{\alpha + \kappa}{2} + i \frac{\beta_2 L}{2!} \frac{\partial^2}{\partial \tau^2} - i \frac{\beta_3 L}{3!} \frac{\partial^3}{\partial \tau^3} + i\delta)E(t, \tau) - \sqrt{\kappa}E_{in} \\ = i\gamma L(|E(t, \tau)|^2 + \tau_R \frac{\partial |E(t, \tau)|^2}{\partial \tau})E(t, \tau). \end{aligned} \quad (1)$$

where $E(t, \tau)$ is the complex slowly varying amplitude of the intracavity electric field, t and τ are slow and fast time of the system. α and κ corresponds to the loss and coupling parameter, β_2 is the GVD value and β_3 is third order dispersion. L is the total MRR length. δ and γ are detuning and nonlinear parameters, respectively. First term on right hand side is Kerr nonlinearity while another contributes to the Raman interactions, where τ_R is the Raman shock time which is partly responsible for self-frequency shift.^{34,37} During the simulation, τ_R is 2.7 fs³⁴ and other material-related parameters are calculated with a finite element solver.³⁴ The β_3 and δ values are used to delicately adjust the global dispersion curve. The calculation is realized through fourth-order Runge-Kutta method.³⁸ The simulated spectrum (red envelope) in Fig. 4(d) is in good agreement with the experimental results (midnight blue) and the inset is the expected soliton pulse inside the MRR.

Theoretically, the DKS could be achieved at any operation temperature provided that the wavelength, detuning and polarization

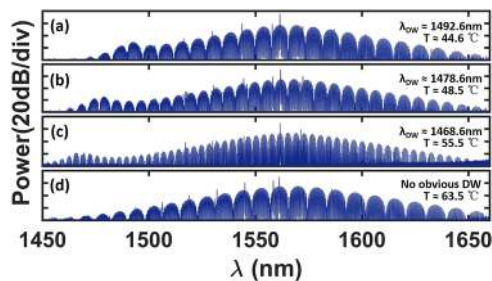


FIG. 5. Different spectra under the temperature of (a) 44.6°C, (b) 48.5°C, (c) 55.5°C, (d) 63.5°C, and the wavelength of DWs are (a) 1492.6 nm (b) 1478.6 nm (c) 1468.6 nm and (d) no obvious DW is observed.

of pump and auxiliary laser are appropriately chosen. The change of temperature could help us to control the center wavelength of DW. Fig. 5 shows the experimental results of four 2-soliton state under $\sim 44.6^\circ\text{C}$, $\sim 48.5^\circ\text{C}$, $\sim 55.5^\circ\text{C}$ and $\sim 63.5^\circ\text{C}$, respectively. The DW is shifted significantly to shorter wavelength with increasing temperature. Remarkably, when the temperature is $\sim 63.5^\circ\text{C}$, the mode-crossing point is tuned out of threshold and no obvious DW is observed, the corresponding spectrum exhibits perfect smooth envelope without any local defects. Our scheme provides a viable and easy way to manipulate the spatial-mode induced DW.

Right now, the number of soliton is not strictly reduced one by one in our experiments ($N, N-1 \dots 1$),²¹ this is attributed to the fact that manually temperature-tuning through a variable-resistor in our current configuration is not precise. We believe that deterministically one-by-one soliton annihilation can be realized once the temperature is tuned at a precision of $\sim 0.02^\circ\text{C}$, which is one order more precise than the SER. This can be realized using programmable digital-to-analog converter to adjust the TEC temperature instead of inexact manual tuning, besides, an on-chip micro-heater could also be a considerable choice for strict deterministic DKSs switching.

In conclusion, we experimentally demonstrate deterministic generation and switching of DKSs in a thermally controlled high-index doped silica MRR with a wavelength-fixed pump. Our scheme is absolutely tuning-speed independent which attributes to the fact that the intra-cavity heat fluctuation is timely balanced by an orthogonally polarized auxiliary laser. Varieties of DKSs and their switching processes are obtained, which is insightful to research the soliton dynamics. Furthermore, the auxiliary laser could be completely filtered out simply using a PBS. By simply determining the DKSs-formed temperature, the center wavelength of DW could be broadly tuned. Our scheme is expected to provide high-performance DKSs in practical applications.

We would like to draw the readers' attention that during the submission of this work, dissipative Kerr soliton generation using an auxiliary laser has recently been demonstrated within silica rod platform independently.^{39,40}

This work was supported by the National Natural Science Foundation of China (NSFC) (Grant No. 61635013, 61675231, 61475188, 61705257), the Strategic Priority Research Program of the Chinese Academy of Sciences (Grant No. XDB24030600). C.-L.

Zou and C.-H. Dong acknowledge the National Key Research and Development Program of China (Grant No. 2016YFA0301303).

REFERENCES

- ¹T. J. Kippenberg, R. Holzwarth, and S. A. Diddams, *Science* **332**, 555–559 (2011).
- ²A. Pasquazi, M. Peccianti, L. Razzari, D. J. Moss, S. Coen, M. Erkintalo, Y. K. Chembo, T. Hansson, S. Wabnitz, and P. Del’Haye, *Phys. Rep.* **729**, 1 (2018).
- ³T. Herr, V. Brasch, J. D. Jost, C. Y. Wang, N. M. Kondratiev, M. L. Gorodetsky, and T. J. Kippenberg, *Nat. Photon.* **8**, 145 (2013).
- ⁴V. Brasch, M. Geiselmann, T. Herr, G. Lihachev, M. H. Pfeiffer, M. L. Gorodetsky, and T. J. Kippenberg, *Science* **351**, 357 (2015).
- ⁵M. Yu, Y. Okawachi, A. G. Griffith, M. Lipson, and A. L. Gaeta, *Optica* **3**, 854 (2016).
- ⁶X. Yi, Q.-F. Yang, K. Y. Yang, M.-G. Suh, and K. Vahala, *Optica* **2**, 1078 (2015).
- ⁷Z. Gong, A. Bruch, M. Shen, X. Guo, H. Jung, L. Fan, X. Liu, L. Zhang, J. Wang, J. Li, J. Yan, and H. X. Tang, *Opt. Lett.* **43**, 4366–4369 (2018).
- ⁸T. J. Kippenberg, A. L. Gaeta, M. Lipson, and M. L. Gorodetsky, *Science* **361**, 567 (2018).
- ⁹M. G. Suh, Q. F. Yang, K. Y. Yang, X. Yi, and K. J. Vahala, *Science* **354**, 600–603 (2016).
- ¹⁰M. Yu, Y. Okawachi, A. G. Griffith, N. Picqué, M. Lipson, and A. L. Gaeta, *Nat. Commun.* **9**, 1869 (2018).
- ¹¹M. G. Suh and K. J. Vahala, *Science* **359**, 884 (2018).
- ¹²P. Trocha, M. Karpov, D. Ganin, M. H. P. Pfeiffer, A. Kordts, S. Wolf, J. Krockenberger, P. Marin-Palomo, C. Weimann, and S. Randel, *Science* **359**, 887 (2018).
- ¹³W. Liang, D. Eliyahu, V. S. Ilchenko, A. A. Savchenkov, A. B. Matsko, D. Seidel, and L. Maleki, *Nat. Commun.* **6**, 7957 (2015).
- ¹⁴P. Marinpalomo, J. N. Kemal, M. Karpov, A. Kordts, J. Pfeifle, M. H. P. Pfeiffer, P. Trocha, S. Wolf, V. Brasch, and M. H. Anderson, *Nature* **546**, 274 (2017).
- ¹⁵Y. Geng, X. Huang, W. Cui, Y. Ling, B. Xu, J. Zhang, X. Yi, B. Wu, S. W. Huang, and K. Qiu, *Opt. Lett.* **43**, 2406 (2018).
- ¹⁶S.-G. Suh, X. Yi, Y.-H. Lai, S. Leifer, I. S. Grudin, G. Vasisht, E. C. Martin, M. P. Fitzgerald, G. Doppmann, J. Wang, D. Mawet, S. B. Papp, S. A. Diddams, C. Beichman, and K. Vahala, *Nat. Photon.* **13**, 23–30 (2019).
- ¹⁷E. Obrzud, M. Rainer, A. Harutyunyan, M. H. Anderson, J. Liu, M. Geiselmann, B. Chazelas, S. Kundermann, S. Lecomte, M. Cecconi, A. Ghedina, E. Molonari, F. Pepe, F. Wildi, F. Bouchy, T. J. Kippenberg, and T. Herr, *Nat. Photon.* **13**, 31–35 (2019).
- ¹⁸C. Bao, Y. Xuan, J. A. Jaramillovillegas, D. E. Leaird, M. Qi, and A. M. Weiner, *Opt. Lett.* **42**, 2519 (2017).
- ¹⁹C. Joshi, J. K. Jang, K. Luke, X. Ji, S. A. Miller, A. Klenner, Y. Okawachi, M. Lipson, and A. L. Gaeta, *Opt. Lett.* **41**, 2565 (2016).
- ²⁰C. Bao, Y. Xuan, D. E. Leaird, S. Wabnitz, M. Hao, and A. M. Weiner, *Optica* **4**, 1011–1015 (2017).
- ²¹H. Guo, M. Karpov, E. Lucas, A. Kordts, M. H. P. Pfeiffer, V. Brasch, G. Lihachev, V. E. Lobanov, M. L. Gorodetsky, and T. J. Kippenberg, *Nat. Phys.* **13**, 94 (2016).
- ²²Y. Geng, M. Liao, H. Zhou, B. Wu, and K. Qiu, in *Nonlinear Optics*, 2017, NMI.4.
- ²³X. Xu, J. Wu, T. G. Nguyen, T. Moein, S. T. Chu, B. E. Little, R. Morandotti, A. Mitchel, and D. J. Moss, *Photon. Res.* **6**, B30 (2018).
- ²⁴W. Wang, Z. Lu, W. Zhang, S. T. Chu, B. E. Little, L. Wang, X. Xie, M. Liu, Q. Yang, L. Wang, J. Zhao, G. Wang, Q. Sun, Y. Liu, Y. Wang, and W. Zhao, *Opt. Lett.* **43**, 2002 (2018).
- ²⁵X. Yi, Q.-F. Yang, K. Y. Yang, and K. Vahala, *Nat. Commun.* **9**, 3565 (2018).
- ²⁶F.-X. Wang, W. Wang, R. Niu, X. Wang, C.-L. Zou, C.-H. Dong, B. E. Little, S. T. Chu, H. Liu, P. Hao, S. Liu, S. Wang, Z.-Q. Yin, D.-Y. He, W. Zhang, W. Zhao, Z.-F. Han, G.-C. Guo, and W. Chen, *arXiv:1812.11415v1* (2019).
- ²⁷W. Wang, W. Zhang, S. T. Chu, B. E. Little, Q. Yang, L. Wang, X. Hu, L. Wang, G. Wang, Y. Wang, and W. Zhao, *ACS Photon.* **4**(6), 1677 (2017).
- ²⁸W. Wang, W. Zhang, Z. Lu, S. T. Chu, B. E. Little, Q. Yang, L. Wang, and W. Zhao, *Photon. Res.* **6**, 363 (2018).
- ²⁹D. C. Cole, E. S. Lamb, P. Del’Haye, S. A. Diddams, and S. B. Scott, *Nat. Photon.* **11**, 671 (2017).
- ³⁰X. Yi, Q.-F. Yang, X. Zhang, K. Y. Yang, X. Li, and K. Vahala, *Nat. Commun.* **8**, 14869 (2017).
- ³¹Q.-F. Yang, X. Yi, K. Y. Yang, and K. Vahala, *Optica* **3**, 1132 (2016).
- ³²X. Liu, C. Sun, B. Xiong, L. Wang, J. Wang, Y. Han, Z. Hao, H. Li, Y. Luo, and J. Yan, *ACS Photon.* **5**(5), 1943 (2018).
- ³³X. Yi, Q.-F. Yang, K. Y. Yang, and K. Vahala, *Opt. Lett.* **41**, 3419 (2016).
- ³⁴Z. Lu, W. Wang, W. Zhang, M. Liu, L. Wang, S. T. Chu, B. E. Little, J. Zhao, P. Xie, X. Wang, and W. Zhao, *Opt. Mater. Express* **8**, 2662 (2018).
- ³⁵G. P. Agrawal, *Nonlinear Fiber Optics* (Academic Press, 2007).
- ³⁶D. Duchesne, M. Ferrera, L. Razzari, R. Morandotti, B. Little, S. T. Chu, and D. J. Moss, *arXiv preprint arXiv:1505.05953* (2015).
- ³⁷M. Karpov, H. Guo, A. Kordts, V. Brasch, M. H. Pfeiffer, M. Zervas, M. Geiselmann, and T. J. Kippenberg, *Phys. Rev. Lett.* **116**, 103902 (2016).
- ³⁸M. Liu, L. Wang, Q. Sun, S. Li, Z. Ge, Z. Lu, W. Wang, G. Wang, W. Zhang, and X. Hu, *Photon. Res.* **6**, 238 (2018).
- ³⁹S. Zhang, J. Silver, L. D. Bino, F. Copie, M. Woodley, G. Ghalanos, A. Svela, N. Moroney, and P. Del’Haye, *arXiv preprint arXiv:1809.06490* (2018).
- ⁴⁰R. Niu, S. Wan, S.-M. Sun, T.-G. Ma, H.-J. Chen, W.-Q. Wang, Z.-Z. Lu, W.-F. Zhang, G.-C. Guo, C.-L. Zou, and C.-H. Dong, *arXiv preprint arXiv:1809.10030* (2018).